Photoredox Catalysis Mediated by Tungsten(0) Arylisocyanides in 1,2-Difluorobenzene

Alexandra T. Barth, Maryann Morales, Jay R. Winkler* and Harry B. Gray*

Beckman Institute, California Institute of Technology, Pasadena, California 91125, United States.

ABSTRACT: We have studied the photochemical cyclization of 1-(2-iodobenzyl)-pyrrole (IBP) and 1-(2-bromobenzyl)-pyrrole (BBP) to 5*H*-pyrrolo[2,1-a]isoindol catalyzed by W(CNDipp)$_6$ (CNDipp = 2,6-diisopropylphenylisocyanide) in 1,2-difluorobenzene (DFB). Irradiation (445 nm) of W(CNDipp)$_6$ (5 mol%) in DFB solution converted 78% of IBP (50 mM) to product after 1 h (16 turnovers). Addition of tetra-*n*-butyl ammonium hexafluorophosphate (TBAPF$_6$) (0.2 M) to the DFB solution led to rapid photoinduced disappearance of W(CNDipp)$_6$ but, remarkably, did not inhibit photochemical cyclization of IBP, indicating that IBP cyclization could be driven by a nonluminescent photocatalyst.

INTRODUCTION

A goal of renewable energy science is replacement of rare metal (Ru, Rh, Ir, Pt) photosensitizers and catalysts with ones containing only earth-abundant elements.[1–17] To achieve this goal, we have synthesized and fully characterized tungsten(0) arylisocyanides whose metal-to-ligand charge-transfer (MLCT) excited states (*W(CNAr)$_6$) are exceptionally strong photoreductants ($E°(W^+/*W^0)$ = −2.2 to −3.0 V vs Fc$^{[+/0]}$).[18–23] We have shown that [*W(CNAr)$_6$] complexes reduce challenging substrates such as anthracene and acetophenone,[20,21] and that their intense visible absorption features and synthetic modularity make them attractive candidates for one- and two-photon photoredox catalysis.[24,25]

Base-promoted homolytic aromatic substitution (BHAS)[26,27] transformations provide a convenient test of photoredox reactivity.[24] In prior work we examined the photochemical conversion of 1-(2-iodobenzyl)-pyrrole (IBP) and 1-(2-bromobenzyl)-pyrrole (BBP) to 5*H*-pyrrolo[2,1-a]isoindol catalyzed by W(CNAr)$_6$ in C_6D_6 solution (Figure 1).[25] With W(CNDipp)$_6$ (CNDipp = 2,6-diisopropylphenylisocyanide) at 5 mol % loading, 1 h of irradiation (6W diode laser, 445 nm) afforded 62% conversion to the cyclized product, corresponding to a turnover number (TON) of 11. Longer irradiation times did not increase turnovers; ^{1}H NMR, UV-visible absorption and luminescence spectra confirmed the conversion of W(CNDipp)$_6$ into photochemically unreactive WI$_2$(CNDipp)$_5$. Our proposed mechanism for W(CNAr)$_6$ catalyzed IDP or BBP cyclization included two critical unproductive pathways stemming from tight ion pairs in benzene solution (Figure 1).[25]

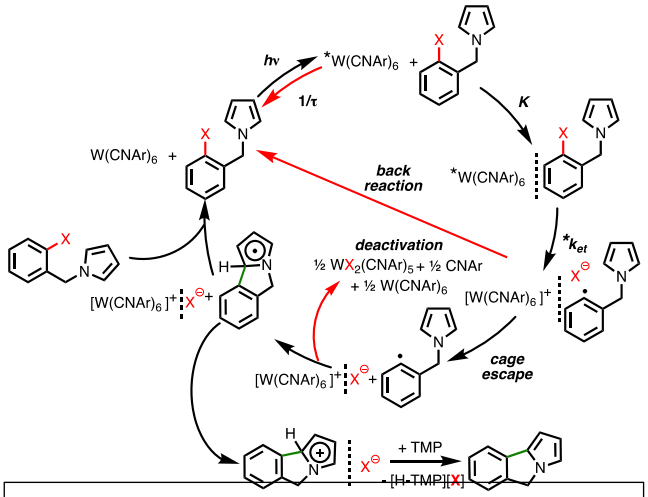

Figure 1. Proposed mechanism for BHAS photoredox catalysis mediated by W(CNAr)$_6$ in benzene solution.[24,25] Red arrows indicate unproductive pathways. Abbreviations include X = Br, I; TMP = 2,2,6,6-tetramethylpiperidine; concerted electron transfer k_{et} ; and equilibrium constant *K*. Ion pairing represented by dashed lines.

Several steps in the proposed mechanism involve ion-pair formation or disappearance, and we suggested that a more polar solvent and/or the addition of electrolyte could alter the balance between productive and unproductive pathways in BHAS photocatalysis with W(CNAr)$_6$.[25] Prior work on *W(CNAr)$_6$ electron-transfer quenching demonstrated that the addition of electrolyte in a low dielectric solvent (THF) produced a dramatic enhancement of the cage-escape yield.[21] We selected 1,2-difluorobenzene (DFB, ε_0 = 13.38[28]) as solvent, and tetra-*n*-butyl ammonium hexafluorophosphate (TBAPF$_6$) as electrolyte to test this hypothesis. We also employed TBA iodide as electrolyte in the IBP reactions.

RESULTS AND DISCUSSION

The first step in the photocatalytic process is electron-transfer (ET) quenching of *W(CNDipp)$_6$ by IBP or BBP. Although the *W(CNAr)$_6$ lifetime decreases by about a factor of 2 when DFB replaces benzene or toluene as solvent, high concentrations of TBAPF$_6$, TBAI, and TMP have no measurable impact on *W(CNAr)$_6$ decay kinetics. The specific rate (k_{obsd}) of *W(CNDipp)$_6$ luminescence decay in DFB solutions varies linearly with IDB or BBP concentration. The second-order rate constants extracted from the kinetics (k_q, Table 1; Tables S1-S5)

Table 1. Luminescence Quenching Kinetics[a]

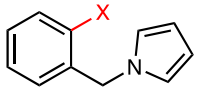

Solvent	X	[Electrolyte]	k_q ($M^{-1}s^{-1}$)[b]	ϕ_q (%)[c]
Benzene	I	-	6.2×10^7	26
DFB	I	-	3.1×10^8	49
DFB	I	0.2 M TBAI	3.5×10^8	51
DFB	I	0.2 M $TBAPF_6$	6.4×10^8	66
Benzene	Br	-	8.6×10^6	5
DFB	Br	-	7.0×10^7	19
DFB	Br	0.2 M $TBAPF_6$	8.1×10^7	20

[a]Quenching experiments performed in deaerated solutions at room temperature. [b]From the slopes of k_{obsd} *vs.* [substrate] plots. [c]Quenching yield with 50 mM substrate.

reveal that DFB produces substantial increases in quenching rates for both the iodo- and bromo-aromatic substrates (Table 1). Addition of $TBAPF_6$ (0.2 M) leads to further rate enhancements. These observations are consistent with increased reaction driving force, owing to stabilization of the ET products in the more polar solvent environment. The larger ET rate constants in DFB also produce substantial increases in yields of quenching products (Table 1).

We then examined the photochemical cyclization reactions of IDB and BBP catalyzed by $W(CNDipp)_6$ in DFB solution. All reactions were performed in the presence of IBP or BBP (50 mM) and a 2-fold excess (100 mM) of 2,2,6,6-tetramethylpiperidine (TMP) to scavenge protons produced in the cyclization reaction. Quantitative product analyses were performed using No-D ^{1}H NMR in DFB.[29] The method was tested by comparing photolysis yields evaluated in C_6H_6 and C_6D_6. Both solvents afforded virtually identical conversion yields and TON values (Table S6).

The most striking difference between $W(CNDipp)_6$ catalyzed IBP cyclization in DFB and C_6D_6 is the conversion rate. Product quantification from ^{1}H NMR afforded comparable reactivity in DFB after 5 min to that in C_6D_6 after 1-h irradiation (Table 2). Although direct kinetics comparisons are difficult, owing to variations in excitation conditions, the reactions clearly proceed much more rapidly in DFB than in C_6D_6. Two factors likely contribute this enhanced photoreactivity. The Stern-Volmer quenching studies reveal a two-fold increase in the yield of ET quenching products in DFB over benzene. Increased ET driving force in the more polar solvent (DFB $\varepsilon_0 = 13.38$[28], benzene $\varepsilon_0 = 2.26$[30]) is the likely explanation for this observation. The second factor is increased cage-escape of ET quenching products, thereby inhibiting the unproductive back reaction. As with reactions conducted

Table 2. Photoredox Catalysis of 1-(2-indobenzyl)-pyrrole Conversion to Cyclized Product

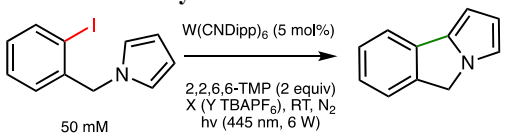

Solvent (X)	[Electrolyte] (Y)	Irrad. Time (min)	Conversion (%)	TON
C_6D_6	-	5	34	7
C_6D_6	-	60	62	11
DFB	-	5	62	13
DFB	-	60	78	16
DFB	-	120	81	17
DFB	0.2 M TBAI	5	68	9
DFB	0.2 M TBAI	60	83	10
DFB	0.2 M TBAI	120	87	11
DFB	0.2 M $TBAPF_6$	5	44	8
DFB	0.2 M $TBAPF_6$	60	67	13
DFB	0.2 M $TBAPF_6$	120	74	14

in C_6D_6, the luminescence (Figure 2), UV-visible (Figure S23), and ^{1}H NMR signatures of $W(CNDipp)_6$ (Figures S83-S86) disappeared after 1-h irradiation in DFB. At lower loadings, however, the catalyst remained active for more than 120 min (Figure 3).

We also examined the effect of dissolved electrolyte on $W(CNDipp)_6$ photoreactions in DFB solution. The presence of TBAI (0.2 M) had little impact on catalysis, and $TBAPF_6$ (0.2 M) produced a modest reduction in the rate of $W(CNDipp)_6$-catalyzed IBP photocyclization (Table 1). More remarkable, however, was the loss of $W(CNDipp)_6$ luminescence after just 10 min of irradiation in the presence of either electrolyte (Figures 2 and S28), indicating that IBP cyclization was driven by a non-luminescent photocatalyst (*vide infra*). UV-visible spectra (Figure S24) and ^{1}H NMR (Figures S89-S91) confirm the disappearance of $W(CNDipp)_6$ from solution.

The high molar extinction coefficient of $W(CNDipp)_6$ (ε_{445nm} = ~55,000 M^{-1} cm^{-1}, Figure S18) prohibited penetration of light into the bulk of the reaction mixture, as demonstrated by precipitation of [H-TMP][I] on the entrance surface of the sample tube. At 5 mol%

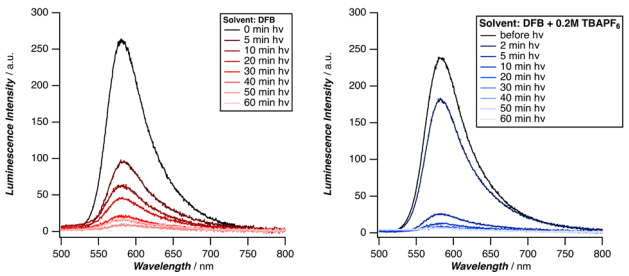

Figure 2. Luminescence spectra of 5 mol% $W(CNDipp)_6$ catalyst, 2 equivalents TMP, and 50 mM IBP in DFB (left). Same conditions with added 0.2 M $TBAPF_6$ (right).

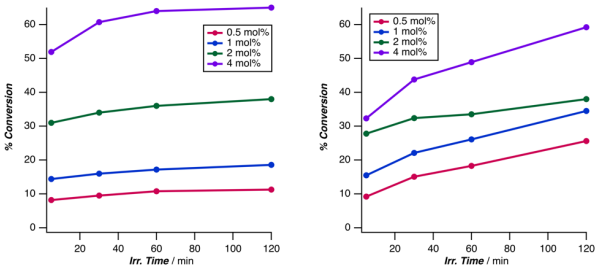

Figure 3. Catalyst loading dependence of substrate conversion to cyclized product: $W(CNDipp)_6$ photocatalyst with, 100 mM TMP, and 50 mM IBP in DFB solution (left). Percent conversion values with addition of 0.2 M $TBAPF_6$ (right).

loading, >95% of the excitation light was absorbed in the first 10 μm of sample. It seemed likely that lowering the catalyst loading would involve more of the sample in catalysis and lead to higher TON values.

Lower catalyst loadings (4, 2, 1, and 0.5 mol%) had little impact on irradiations in DFB. Conversion to substrate ceased after 1-2 h of irradiation (Figure 3) with TONs in the range of 16-22. With 0.2 M $TBAPF_6$ in DFB, however, conversion to product was initially slower, but continued to increase roughly linearly with time after 2 h of irradiation (Figure 3). Moreover, lower catalyst loadings produced higher TON values: after 2-h irradiation at 0.5 mol% catalyst loading the TON was 51; after 24 h the TON was 179, corresponding to 89% substrate conversion.

We extended our work in DFB/$TBAPF_6$ solutions to include the BBP substrate. In our prior study, we found that ca. 10 mol% $W(CNDipp)_6$ loading in C_6D_6 afforded 14% substrate conversion (1.2 TON) after 12-h irradiation.[25] Experiments in DFB with ca. 5 mol% catalyst loading gave 6% conversion (1.5 TON) after 1-h irradiation, and 16.8% conversion (3.5 TON) after 24-h irradiation. Upon addition of 0.2 M $TBAPF_6$, we found 8.4% conversion (1.5 TON) after 1-h irradiation and 27.7% conversion (5.0 TON) after 24-h irradiation. In both studies, $W(CNDipp)_6$ luminescence persisted after 1-h

Table 3. Photoredox Catalysis of 1-(2-bromobenzyl)-pyrrole Conversion to Cyclized Product

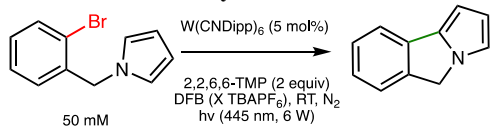

[$TBAPF_6$] (X)	Irrad. Time (h)	Conversion (%)	TON
-	1	6.0	1.5
-	2	9.0	1.9
-	24	16.8	3.5
0.2 M	1	8.4	1.5
0.2 M	2	12.4	2.2
0.2 M	24	27.7	5.0

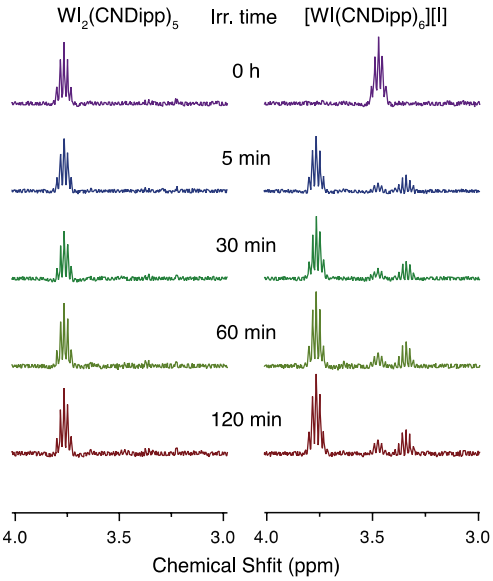

Figure 4. ^1H NMR spectra (methine resonances) of $WI_2(CNDipp)_5$ (left, 3.77 ppm) and $[WI(CNDipp)_6]I$ (right, 3.47 ppm) after irradiation with 1-(2-iodobenzyl)-pyrrole in DFB solution. Upon irradiation, $[WI(CNDipp)_6]I$ liberates CNDipp (3.39 ppm) with formation of $WI_2(CNDipp)_5$.

irradiation, indicating greatly reduced catalyst degradation (Figures S26, S27).

In prior work, we identified $WI_2(CNDipp)_5$ as the deactivation product of photocatalysis in C_6D_6. This seven-coordinate W(II) complex, or a related six-coordinate W(II) species, $[WI(CNDipp)_6]^+$, could be a photocatalyst in DFB. Irradiation of $[WI(CNDipp)_6]I$ in DFB with IBP (50 mM) led to rapid (5 min) formation of $WI_2(CNDipp)_5$, the liberation of CNDipp, and only trace product formation (Figure 4), thereby eliminating the six-coordinate W(II) complex as a candidate for the nonluminescent photcatalyst. After 1-h irradiation of $WI_2(CNDipp)_5$ with IBP in DFB, however, we found 4% conversion to cyclized product (1 TON); and the conversion was 12% (3 TON) after 1-h irradiation with 0.2 M $TBAPF_6$ in solution. We conclude that $WI_2(CNDipp)_5$ photocatalyzes IBP cyclization, although its activity is markedly lower than that of electronically excited $W(CNDipp)_6$ in DFB solutions.

CONCLUDING REMARKS

We have shown that substrate conversion to cyclized product was enhanced when $W(CNDipp)_6$-mediated photoredox catalysis of BHAS reactions was run in a solvent (DFB) more polar than benzene. Although the reaction was somewhat slower with addition of 0.2 M $TBAPF_6$, catalytic activity continued well beyond a TON value of 20, reaching 179 TON after 24-h irradiation in DFB solution.

There is another advantage of employing DFB as the BHAS reaction solvent, namely, that photogeneration of $WI_2(CNDipp)_5$ does not terminate catalysis, in striking contrast to the outcome in benzene.

ASSOCIATED CONTENT

Supporting Information. The Supporting Information is available free of charge at http://pubs.acs.org.

Experimental details; characterization data; spectroscopic data (^{1}H and ^{13}C NMR, IR, UV–visible absorbance, steady-state luminescence, time-resolved luminescence).

AUTHOR INFORMATION

Corresponding Authors

Jay R. Winkler − Beckman Institute, California Institute of Technology (Caltech), Pasadena, California 91125, United States; orcid.org/0000-0002-4453-9716;
Email: winklerj@caltech.edu

Harry B. Gray − Beckman Institute, California Institute of Technology (Caltech), Pasadena, California 91125, United States; orcid.org/0000-0002-7937-7876;
Email: hbgray@caltech.edu

Authors

Alexandra T. Barth − Beckman Institute, California Institute of Technology (Caltech), Pasadena, California 91125, United States; orcid.org/ 0000-0002-1813-4029

Maryann Morales − Beckman Institute, California Institute of Technology (Caltech), Pasadena, California 91125, United States; orcid.org/0000-0022-1778-8901

Author Contributions

All authors have given approval to the final version of the manuscript.

Funding Sources

We thank the National Science Foundation (CHE-1763429) and the Caltech Beckman Institute Laser Resource Center supported by the Arnold and Mabel Beckman Foundation. A.T.B. acknowledges a National Science Foundation Graduate Research Fellowship (NSF Grant No. DGE-1745301).

ACKNOWLEDGMENT

We thank Javier Fajardo, Jr. for helpful discussions.

REFERENCES

(1) Shing Cheung, K. P.; Sarkar, S.; Gevorgyan, V. Visible Light-Induced Transition Metal Catalysis. *Chem. Rev.* **2021**. https://doi.org/10.1021/acs.chemrev.1c00403.

(2) Shaw, M. H.; Twilton, J.; MacMillan, D. W. C. Photoredox Catalysis in Organic Chemistry. *J. Org. Chem.* **2016**, *81* (16), 6898–6926. https://doi.org/10.1021/acs.joc.6b01449.

(3) Prier, C. K.; Rankic, D. A.; MacMillan, D. W. C. Visible Light Photoredox Catalysis with Transition Metal Complexes: Applications in Organic Synthesis. *Chem. Rev.* **2013**, *113* (7), 5322–5363. https://doi.org/10.1021/cr300503r.

(4) Gray, H. B. Powering the Planet with Solar Fuel. *Nature Chemistry* **2009**, *1* (1), 7–7. https://doi.org/10.1038/nchem.141.

(5) Lewis, N. S.; Nocera, D. G. Powering the Planet: Chemical Challenges in Solar Energy Utilization. *Proc Natl Acad Sci USA* **2006**, *103* (43), 15729. https://doi.org/10.1073/pnas.0603395103.

(6) Hunter, B. M.; Gray, H. B.; Müller, A. M. Earth-Abundant Heterogeneous Water Oxidation Catalysts. *Chem. Rev.* **2016**, *116* (22), 14120–14136. https://doi.org/10.1021/acs.chemrev.6b00398.

(7) Hernandez-Perez, A. C.; Collins, S. K. Heteroleptic Cu-Based Sensitizers in Photoredox Catalysis. *Acc. Chem. Res.* **2016**, *49* (8), 1557–1565. https://doi.org/10.1021/acs.accounts.6b00250.

(8) Reiser, O. Shining Light on Copper: Unique Opportunities for Visible-Light-Catalyzed Atom Transfer Radical Addition Reactions and Related Processes. *Acc. Chem. Res.* **2016**, *49* (9), 1990–1996. https://doi.org/10.1021/acs.accounts.6b00296.

(9) Larsen, C. B.; Wenger, O. S. Photoredox Catalysis with Metal Complexes Made from Earth-Abundant Elements. *Chem. Eur. J.* **2018**, *24* (9), 2039–2058. https://doi.org/10.1002/chem.201703602.

(10) He, J.; Chen, C.; Fu, G. C.; Peters, J. C. Visible-Light-Induced, Copper-Catalyzed Three-Component Coupling of Alkyl Halides, Olefins, and Trifluoromethylthiolate To Generate Trifluoromethyl Thioethers. *ACS Catal.* **2018**, *8* (12), 11741–11748. https://doi.org/10.1021/acscatal.8b04094.

(11) Zhang, Y.; Petersen, J. L.; Milsmann, C. A Luminescent Zirconium(IV) Complex as a Molecular Photosensitizer for Visible Light Photoredox Catalysis. *J. Am. Chem. Soc.* **2016**, *138* (40), 13115–13118. https://doi.org/10.1021/jacs.6b05934.

(12) Zhang, Y.; Lee, T. S.; Favale, J. M.; Leary, D. C.; Petersen, J. L.; Scholes, G. D.; Castellano, F. N.; Milsmann, C. Delayed Fluorescence from a Zirconium(IV) Photosensitizer with Ligand-to-Metal Charge-Transfer Excited States. *Nature Chemistry* **2020**, *12* (4), 345–352. https://doi.org/10.1038/s41557-020-0430-7.

(13) Qiao, Y.; Schelter, E. J. Lanthanide Photocatalysis. *Acc. Chem. Res.* **2018**, *51* (11), 2926–2936. https://doi.org/10.1021/acs.accounts.8b00336.

(14) Büldt, L. A.; Guo, X.; Vogel, R.; Prescimone, A.; Wenger, O. S. A Tris(Diisocyanide)Chromium(0) Complex Is a Luminescent Analog of Fe(2,2′-Bipyridine)$_3^{2+}$. *J. Am. Chem. Soc.* **2017**, *139* (2), 985–992. https://doi.org/10.1021/jacs.6b11803.

(15) Büldt, L. A.; Guo, X.; Prescimone, A.; Wenger, O. S. A Molybdenum(0) Isocyanide Analogue of Ru(2,2′-Bipyridine)$_3^{2+}$: A Strong Reductant for Photoredox Catalysis. *Angewandte Chemie International Edition* **2016**, *55* (37), 11247–11250. https://doi.org/10.1002/anie.201605571.

(16) Bilger, J. B.; Kerzig, C.; Larsen, C. B.; Wenger, O. S. A Photorobust Mo(0) Complex Mimicking [Os(2,2′-Bipyridine)$_3$]$^{2+}$ and Its Application in Red-to-Blue Upconversion. *J. Am. Chem. Soc.* **2021**, *143* (3), 1651–1663. https://doi.org/10.1021/jacs.0c12805.

(17) Yu, D.; To, W.-P.; Tong, G. S. M.; Wu, L.-L.; Chan, K.-T.; Du, L.; Phillips, D. L.; Liu, Y.; Che, C.-M. Luminescent Tungsten(vi) Complexes as Photocatalysts for Light-Driven C–C and C–B Bond Formation Reactions. *Chem. Sci.* **2020**, *11* (25), 6370–6382. https://doi.org/10.1039/D0SC01340D.

(18) Wegeberg, C.; Häussinger, D.; Wenger, O. S. Pyrene-Decoration of a Chromium(0) Tris(Diisocyanide) Enhances Excited State Delocalization: A Strategy to Improve the Photoluminescence of 3d6 Metal Complexes. *J. Am. Chem. Soc.* **2021**, *143* (38), 15800–15811. https://doi.org/10.1021/jacs.1c07345.

(19) Fajardo, J.; Schwan, J.; Kramer, W. W.; Takase, M. K.; Winkler, J. R.; Gray, H. B. Third-Generation W(CNAr)$_6$ Photoreductants (CNAr = Fused-Ring and Alkynyl-Bridged Arylisocyanides). *Inorg. Chem.* **2021**, *60* (6), 3481–3491. https://doi.org/10.1021/acs.inorgchem.0c02912.

(20) Sattler, W.; Henling, L. M.; Winkler, J. R.; Gray, H. B. Bespoke Photoreductants: Tungsten Arylisocyanides. *J. Am. Chem. Soc.* **2015**, *137* (3), 1198–1205. https://doi.org/10.1021/ja510973h.

(21) Sattler, W.; Ener, M. E.; Blakemore, J. D.; Rachford, A. A.; LaBeaume, P. J.; Thackeray, J. W.; Cameron, J. F.; Winkler, J. R.; Gray, H. B. Generation of Powerful Tungsten Reductants by Visible Light Excitation. *J. Am. Chem. Soc.* **2013**, *135* (29), 10614–10617. https://doi.org/10.1021/ja4047119.

(22) Kvapilová, H.; Sattler, W.; Sattler, A.; Sazanovich, I. V.; Clark, I. P.; Towrie, M.; Gray, H. B.; Záliš, S.; Vlček, A. Electronic Excited States of Tungsten(0) Arylisocyanides. *Inorg. Chem.* **2015**, *54* (17), 8518–8528. https://doi.org/10.1021/acs.inorgchem.5b01203.

(23) Mann, K. R.; Cimolino, M.; Geoffroy, G. L.; Hammond, G. S.; Orio, A. A.; Albertin, G.; Gray, H. B. Electronic Structures and Spectra of Hexakisphenylisocyanide Complexes of Cr(0), Mo(0), W(0), Mn(I), and Mn(II). *Inorganica Chimica Acta* **1976**, *16*, 97–101. https://doi.org/10.1016/S0020-1693(00)91697-9.

(24) Herr, P.; Glaser, F.; Büldt, L. A.; Larsen, C. B.; Wenger, O. S. Long-Lived, Strongly Emissive, and Highly Reducing Excited States in Mo(0) Complexes with Chelating Isocyanides. *J. Am. Chem. Soc.* **2019**, *141* (36), 14394–14402. https://doi.org/10.1021/jacs.9b07373.

(25) Fajardo, J.; Barth, A. T.; Morales, M.; Takase, M. K.; Winkler, J. R.; Gray, H. B. Photoredox Catalysis Mediated by Tungsten(0) Arylisocyanides. *J. Am. Chem. Soc.* **2021**. https://doi.org/10.1021/jacs.1c07617.

(26) Studer, A.; Curran, D. P. Organocatalysis and C-H Activation Meet Radical- and Electron-Transfer Reactions. *Angewandte Chemie International Edition* **2011**, *50* (22), 5018–5022. https://doi.org/10.1002/anie.201101597.

(27) Studer, A.; Curran, D. P. The Electron Is a Catalyst. *Nature Chemistry* **2014**, *6* (9), 765–773. https://doi.org/10.1038/nchem.2031.

(28) Mansingh, A.; McLay, D. B. Dielectric Relaxation of Dihalobenzenes. III. Pure Liquids. *J. Chem. Phys.* **1971**, *54* (8), 3322–3325. https://doi.org/10.1063/1.1675346.

(29) Hoye, T. R.; Eklov, B. M.; Ryba, T. D.; Voloshin, M.; Yao, L. J. No-D NMR (No-Deuterium Proton NMR) Spectroscopy: A Simple Yet Powerful Method for Analyzing Reaction and Reagent Solutions. *Org. Lett.* **2004**, *6* (6), 953–956. https://doi.org/10.1021/ol049979+.

(30) Mardolcar, U. V.; de Castro, C. A. N.; Santos, F. J. V. Dielectric Constant Measurements of Toluene and Benzene. *Fluid Phase Equilibria* **1992**, *79*, 255–264. https://doi.org/10.1016/0378-3812(92)85135-U.

For Table of Contents Only

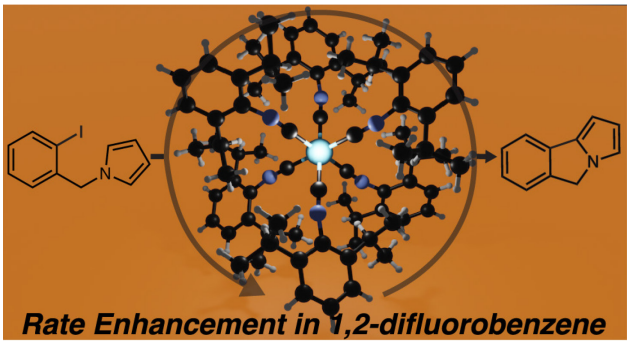

Synopsis

Photochemical base-promoted homolytic aromatic substitution catalyzed by tungsten(0) arylisocyanide complexes is faster in 1,2-difluorobenzene than in benzene. Higher electron-transfer quenching rates and greater cage-escape yields of ionic products in the more polar solvent contribute to the enhanced reactivity.